PROCEEDINGS OF SCIENCE

Robust and Non-destructive Readout Card Installation Algorithm for MicroMegas Modules Cosmic Ray Tests

Mikhail Demichev[a,*]

[a] *JINR,*
Joliot-Curie 6, Dubna, Russia

E-mail: mdemichev@jinr.ru

MicroMegas modules of type LM2 for the ATLAS Muon Spectrometer upgrade were assembled and tested in JINR. The tests at the cosmic stand included installation of readout cards to collect cosmic muon data. A dedicated card installation algorithm was developed to keep electronics from electrostatic and mechanical damage. The examples of module cosmic test results such as efficiency maps and data variation with ambient parameters are presented.

11th International Conference of the Balkan Physical Union (BPU11),
28 August - 1 September 2022
Belgrade, Serbia

*Speaker

PoS(BPU11)090

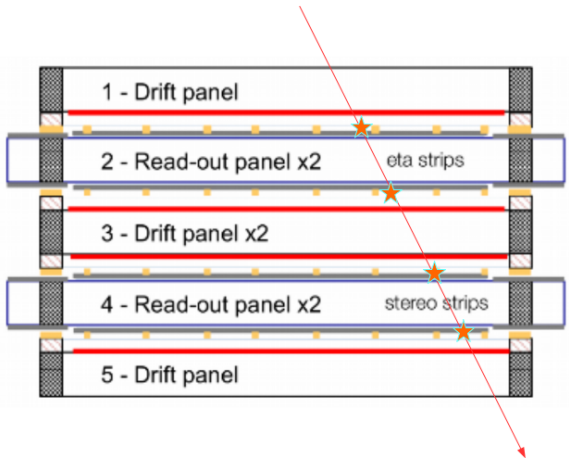

Figure 1: Layout of the MicroMegas module.

1. Introduction

New Small Wheels are the proposed upgrade [1] of ATLAS Muon Spectrometer for higher luminosity LHC runs. New Small Wheels are inner endcap parts of MS about 10m in diameter and are assembled from 8 smaller and 8 larger wedges in CERN construction area. Each wedge consists of eight stacked layers of each of the two detector types. Small-strip Thin Gap Chambers (sTGC) are fast trigger and tracking detectors while the MicroMegas (MM) are precision coordinate trackers. Each NSW wedge is subdivided into detector modules of different types.

MicroMegas (Micro-mesh Gaseous Structure) is an advanced development of wire-chamber tracking detector technology [2]. Conductive mesh divides gas gap into drift space and amplification region with larger electric field. Charged particles traversing the drift space ionize the gas. The electrons drift towards the mesh. The electron avalanche takes place in the amplification region, immediately above the read-out electrode, giving electric signal via capacitive coupling. Resistive layer stops avalanche development into continuous discharge. The layout of a single MM module is shown on the Fig. 1 with a muon track giving charge deposits in the gas volumes.

The type LM2 of MM modules were produced in cooperation between AUoT(Greece) and JINR(Dubna) groups. Drift panels with conductive mesh attached were produced in AUoT, the readout panels were glued in JINR [3]. Each module after assembly from the panel stack was verified in Dubna for geometry alignment, tested for high voltage stability and gas leakage. Finally a physical test at the cosmic stand was done including installation of multichannel readout cards with 8xVMM3 ASICs [4]. The goals of cosmic test were to find and fix the potential problems with electronics installation, to observe a long-term high-voltage stability of the module and to measure the module's efficiency map from tracking.

2. Installation Algorithm and Operational Problems

The readout cards (ROCs) are thick multilayer printed circuit boards with a high density of conductors and components, see Fig. 2. The analog part of the ROC or the so-called signal edge is the area densely filled with SMD components of 0.5×1.0 mm size which are NUP4114

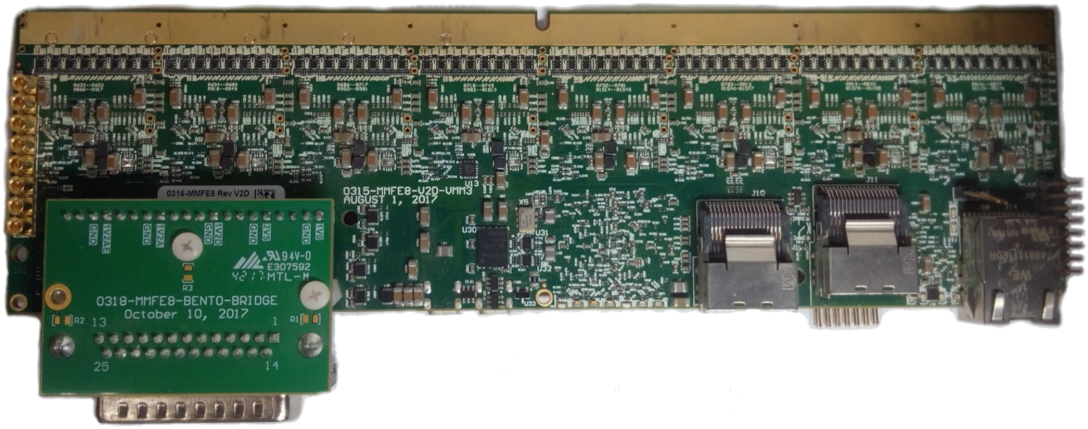

Figure 2: Readout card (ROC) with signal edge (top) and digital edge (bottom).

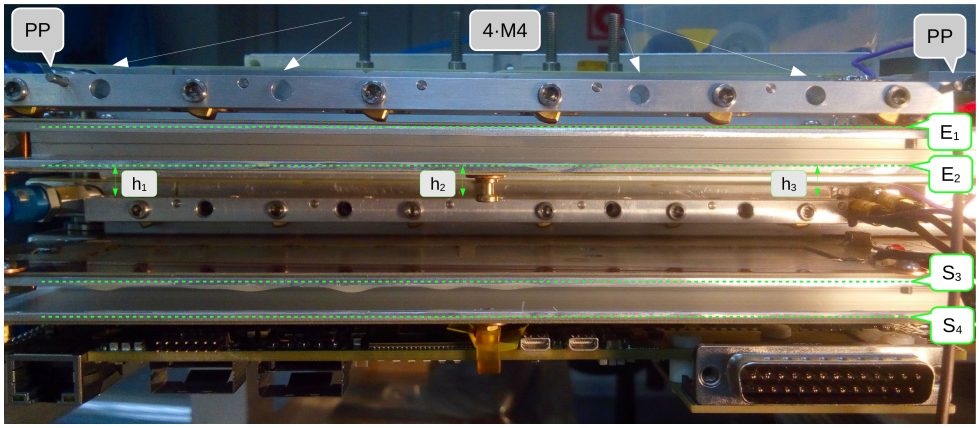

Figure 3: Compression bar with M4 screws, clearance measurements and installed ROC.

ESD protection diode arrays in a compact package and an additional pair of resistors and zener diodes for discharge protection. Care must be taken when handling the ROC during installation, as these protective components can be easily detached due to excessive deformation of the card. Since the operating voltage point of the gaseous particle detector is close to the discharge region, occasional discharges are to be expected. The duration of the discharge inside the detector is limited by the integrated resistive strip coating. Despite this, if the channel protection components are mechanically damaged, the channel will eventually burn out due to discharges.

The bottom digital edge of the ROC has connectors for power, trigger and clock inputs, and a Gigabit Ethernet data output. The digital edge must be fixed with a plastic clamp in the middle to a dedicated stand on the edge of the detector to relieve the mechanical stress of the ROC from power adapter board and wires.

To establish contact between the MicroMegas readout strips and the readout card channels an elastomeric band with conductive microwires is used – a zebra connector. Two zebra connectors are placed in a spacer holder attached to the signal edge of the ROC. Installed inside holder the zebras protrude from it by ≈ 0.1 mm, so the connection retains some flexibility.

The compression bar (CB) is used to apply pressure on the ROC, required to establish electrical

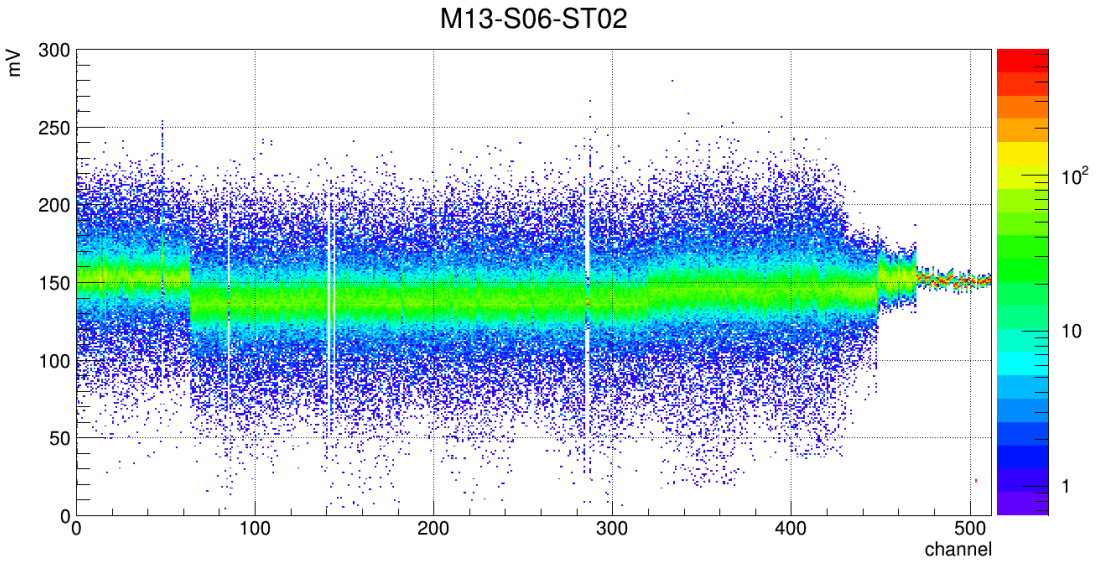

Figure 4: Pedestal calibration run example.

contact between the ROC, the zebra and the detector strips, for which a certain torque is applied to the cams of the CB. The CB has six rotating eccentric cams with a stepped helical surface, two precise pins (PP) for proper positioning on the edge of the drift panel and four holes for M4 screws to secure it, as shown on the top of Fig. 3. In addition, the middle of Fig. 3 shows the installed CB for the second eta readout panel, located between the cooling pipe and the drift HV connectors, as well as the installed ROC at the bottom.

Readout card installation procedure should have been a routine task:

1. A brass stand with a ⌀4 mm copper washer is installed at the edge of the readout panel.
2. The CB is mounted on the drift panel so that its precise pins fit into their respective apertures.
3. The compression bar is secured with four M4 screws to the drift panel.
4. All six CB cams are turned away from the strips to make enough room for ROC installation.
5. The ROC contacts, zebra pads, and module readout strips are cleaned with isopropanol.
6. The ROC is inserted under CB so that corresponding dowel pin fits into the notch in the card.
7. CB cams are locked in order 3 – 4 – 2 – 5 – 1 – 6 with increasing torque but not exceeding the torque limit of 25 N·cm.
8. The digital edge of the ROC is attached to the stand by a plastic clamp.
9. The propagation of signal from the readout strips to the ROC channels via zebra connectors is verified.

The connection quality is checked by pedestal calibration runs. The pedestal is the output voltage level corresponding to zero input charge with a typical value about 170 mV for the VMM3. An unconnected channel on a properly powered and grounded readout card has a typical pedestal noise less than 2 mV RMS for a selected operating gain of 9 mV/fC (millivolts per femtocoulomb). Electrical contact with the strip adds the capacitance of the strip to the capacitance of the input channel thereby increasing the amount of noise in the pedestal up to 10 mV RMS. Thus connected and unconnected strips can be easily distinguished. On the Fig. 4, three dead channels can be

observed around channel number 140 as well as two consecutive unconnected strips around channel 290 which actually should be connected. There is no connection in the channel range 470-512, since these strips are not implemented at the edge of the module.

In case of connection failure it was suggested to unlock the CB and lock it again and then to replace zebra connectors, compression bars, readout cards one by one. After every iteration the readout card must be reinstalled and the connection test repeated.

Although the initial installation procedure was quite straightforward, it did not answer the question what to do if the quality of the connection after several iterations was still unacceptable. It was not an option to override the torque limit as it resulted in permanent damage to the input channel circuits due to the deformation of the ROC.

3. Installation Algorithm Development

Over time, it became apparent that when CB happened to be perfectly parallel to the readout plane, the installation procedure took one or at most two iterations, provided that the dowel pin was straight and reached the CB and there were no blocking parts around the ROC. In addition, it was experimentally found that if the minimal clearance between the CB and the readout plane is less than 9.5 mm, then the cam in this place does not extend to a sufficient length out of CB and cannot be fixed on its first step.

The alignment of the compression bars was introduced at the stage of the preparing the module for testing. The clearances between CB and the readout panel were measured in three positions h_1, h_2, h_3 at the edges of CB and in the middle, see Fig. 3. It was essential to identify the reason why the clearances were reduced. This could happen both due to the offset of the holes for the precise pins and due to the displacement of the holes for the M4 screws.

The compression bar was loosened and the clearance measurements were repeated. If there was no improvement, then the reason was an offset hole for one of the precise pins. Otherwise, the hole for the M4 screw was displaced and it was required to select a specially produced screw with a shortened thread length and a narrow shank. The loosened CB held only on its precision pins has some elastic degree of freedom so that a 9.5 mm calibrated bar could be put under it using it as a crowbar for spreading. Then the CB was fixed with M4 screws, if necessary using special screws, and the calibrated bar was pulled out. After that clearances h_1, h_2, h_3 were measured again and the minimum distance was expected to to increase. Generally, a narrow shank screw provided enough space to alter the position of the CB. At the same time, cases when the hole for the precise pin was moderately displaced, although rare, required repair.

If the minimum clearance requirement has already been met, it may be still mandatory to raise either the middle or the corner of the compression bar. To do this, the calibration bar was inserted end-to-end there, adding the required number of shims to obtain the desired clearance. Then again the compression bar was fixed with M4 screws, the calibrated bar was pulled out, and clearance measurements were taken.

The explanation for the alignment procedure lies in the design of the CB cam, which has a stepped helical surface protruding from the CB by exactly 0.2 mm at each step. However, there is a small edge between each two successive steps on the cam, and the position of the cam when it stops on this edge was found undesirable. When the CB is misaligned, one or even two of the six cams

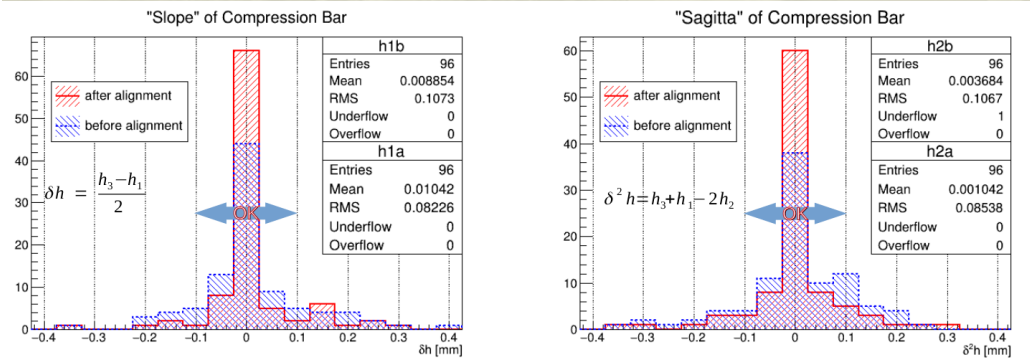

Figure 5: Measured slope and sagging of installed compression bars.

were locked on its edges, and not on the surface of the step. On the other hand, rounded stepless cams have been found to unlock on their own and therefore not recommended for use in production.

The degree of parallelism of the CB to the detector plane is conveniently expressed in terms of slope and sagging calculated from the clearances h_1, h_2, h_3. If, after alignment, the slope and sagging were within a tolerance of 0.1 mm, then such an alignment was considered satisfactory. The alignment effect can be seen in Fig. 5 in reduced variance of the red (after alignment) distributions compared to the blue (before alignment) distributions.

By design, the digital side of the ROC should be fastened with plastic clamp to a small brass support or stand mounted on the edge of the readout panels, see Fig. 6. This was done after the signal side of the ROC was already fixed by the cams of the CB. However, clamping the readout card should cause no additional deformation, as this affects the quality of contact between the zebra connectors and the strips. Excessive deformation of the ROC can even damage the small components on it. So the idea was to measure and maintain the clearance between the signal plane and the outer edge of the ROC. To achieve this the conventional brass stands were not always the best choice.

The brass stand had a typical height of 5.5 mm and together with a ⌀4 mm copper washer 0.80 – 0.85 mm gave a total base height of 6.3 – 6.35 mm. The actual clearance between the ROC and the edge of the readout panel after locking the compression bar could be less than or greater than this base value of 6.3 mm, see Fig. 7, left.

If the clearance between the ROC and the readout panel was less than the base height, a flattened washer up to 0.2 mm high was used instead of the conventional one.

If the clearance was in the range of 6.3 – 6.9 mm, the gap between the ROC and the brass stand was filled with tiny shims made of 0.2 mm thick copper foil. The plastic clamp is elastic enough, so up to 3 such shims can be used, as shown by the dashed blue vertical lines on Fig. 7.

In case the clearance was greater than 6.9 mm a ⌀2.5 × 15 mm screw with a ⌀5.0 × 6.5 mm bushing had to be used instead of the brass stand and the clamp. The brass bushings were machined in a small batch specifically for the ROC installation. Additional copper washers could be used as spacers. The clearance measurement was repeated after clamping the digital edge of the ROC. It had been experimentally established that the clearance change after clamping should be within a tolerance of 0.2 mm, see Fig. 7, on the right.

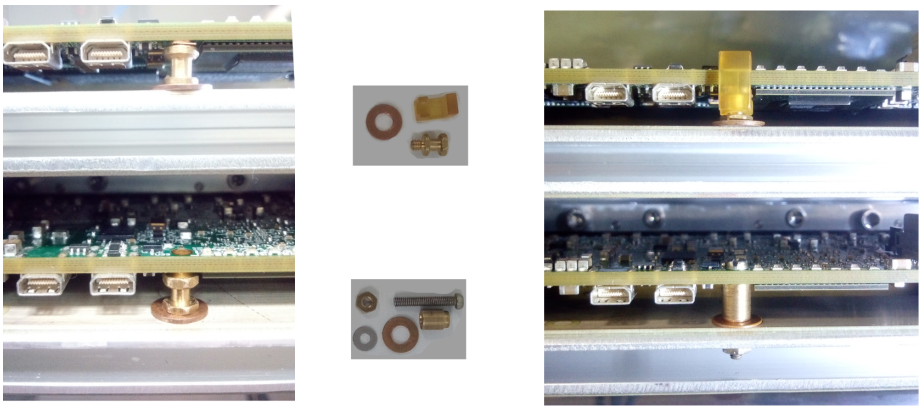

Figure 6: Left: the gap between the ROC and support stand. Right: selection of the type of mounting kit.

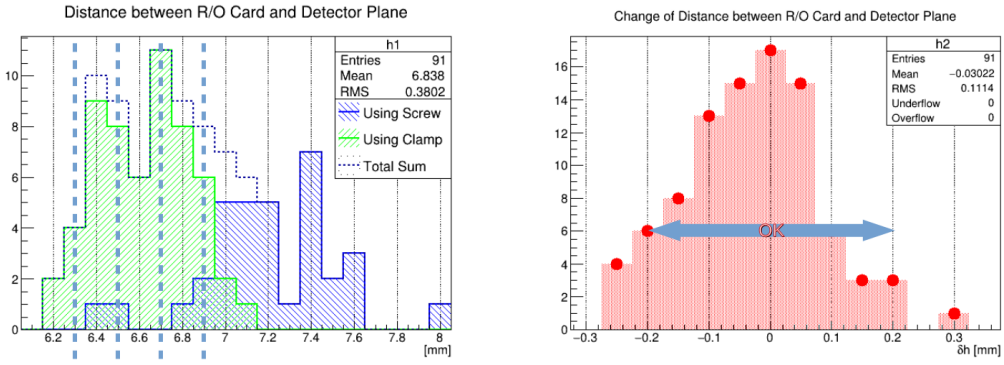

Figure 7: The measured clearance between the ROC and the readout panel before clamping, as well as the change in this clearance after clamping.

Both the CB alignment procedure and the choice of clamping kit, in addition to the original algorithm, gave us a reproducible installation technique. This allowed us to step up from using exclusive personal experience to a robust method so that more staff members can be trained thereby reducing installation time.

4. Cosmic Tests Results

A straight track in space can be specified by five independent parameters. They are the three coordinates of some chosen point which belongs to a track and two angles, zenith and azimuthal, for a track direction. Consider a straight muon track passing through the layers of MicroMegas detector. Here precision coordinate Y in channel numbers is across the strips, auxiliary coordinate X in *mm* is along eta strips and Z is perpendicular to readout panel. We choose a point where the track crosses the first detector layer and take its Z-coordinate for zero. This leaves us with four actual track parameters (X_0, Y_0, θ, ϕ). The track crosses four signal layers E_1, E_2, S_3, S_4 activating four strips which we know by layer and by their number. Here stereo strips S_3, S_4 are rotated with respect to eta strips E_1, E_2 by a small stereo angle $\alpha = 1.5°$ in opposite directions. Strip numbers can be converted to the Y-coordinate as the strip pitch is known, so we end up with four independent strip coordinates $(Y_{E1}, Y_{E2}, Y_{S3}, Y_{S4})$. This is enough to reconstruct initial four straight track parameters.

To calculate efficiency in a particular point of the given 'probe' detector layer a hit-and-miss method is used. At first all of the tracks passing through this point are selected. For each track a check is performed if the probe detector layer counted at this point (hit) or did not count (miss). Then the efficiency estimate will be the number of hits divided by total number of hits and misses, see equation 1,

$$\varepsilon(X,Y) = \frac{N_{hit}(X,Y)}{N_{hit} + N_{miss}}. \tag{1}$$

To continue the track parameters should be determined. As we have no external tracker we have to choose three other MM module layers as a tracker calling them the 'reference' layers. This leaves us only with three independent strip number measurements while the fourth if exists is used for probe layer efficiency measurement. An approximation is required to get information from underdetermined system. Assume that auxiliary track coordinate X remains the same for all detector layers. That is justified by the fact that the detector resolution for X-coordinate is ≈ 20 times worse than for precise Y-coordinate. Effectively we are able to measure only three independent track parameters (X_0, Y_0, θ^*). The azimuthal angle is missing and the zenith angle $\theta^* \sim Y_{E2} - Y_{E1}$ is measured now in $YZ-$ plane.

In a real detector the cloud of initial ionization around the track direction experiences charge drift so after gas amplification the charge is distributed between several adjacent strips the so-called strip cluster. A weighted average is taken to find cluster barycenter where hit weight is a charge collected from each strip of a cluster.

The track reconstruction algorithm builds clusters from consequent hits in one layer with a single strip gap allowed for a cluster. Assuming that cluster barycenter coordinates Y_{E1}, Y_{E2}, Y_{S3}, Y_{S4} in eta and stereo layers 1-4 belong to the same straight track they are connected together with system of equations 2 within the aforementioned approximation:

$$\begin{cases} Y_{S3} = Y_{E1} + 2 \cdot (Y_{E2} - Y_{E1}) + \Delta Y \\ Y_{S4} = Y_{E1} + 3 \cdot (Y_{E2} - Y_{E1}) - \Delta Y \end{cases}, \text{where } \Delta Y = X\, tan(\alpha) \approx 0.0262 \cdot X \tag{2}$$

For stereo strips the actual strip number hit by a track varies by an offset ΔY from which an auxiliary X coordinate can be calculated.

We can rewrite this system of equations 2 to calculate the expected Y hit position in the probe layer using only Y-coordinates of barycenters from reference layers clusters, altogether with approximate X-coordinate, see equations 3-6.

$$Y_{E1}^{exp} = 1/3\ (5Y_{E2} - Y_{S3} - Y_{S4}),\ X = 1/3\ (Y_{E2} - 2Y_{S3} + Y_{S4})\ \frac{1}{tan(\alpha)} \tag{3}$$

$$Y_{E2}^{exp} = 1/5\ (3Y_{E1} + Y_{S3} + Y_{S4}),\ X = 1/5\ (Y_{E1} - 3Y_{S3} + 2Y_{S4})\ \frac{1}{tan(\alpha)} \tag{4}$$

$$Y_{S3}^{exp} = -3Y_{E1} + 5Y_{E2} - Y_{S4},\ X = (2Y_{E1} - 3Y_{E2} + Y_{S4})\ \frac{1}{tan(\alpha)} \tag{5}$$

$$Y_{S4}^{exp} = -3Y_{E1} + 5Y_{E2} - Y_{S3},\ X = (Y_{E1} - 2Y_{E2} + Y_{S3})\ \frac{1}{tan(\alpha)} \tag{6}$$

If the probe layer has any cluster with a barycenter in the proximity of expected hit position, a hit efficiency counter there is increased by one, otherwise a miss counter is increased by one. The

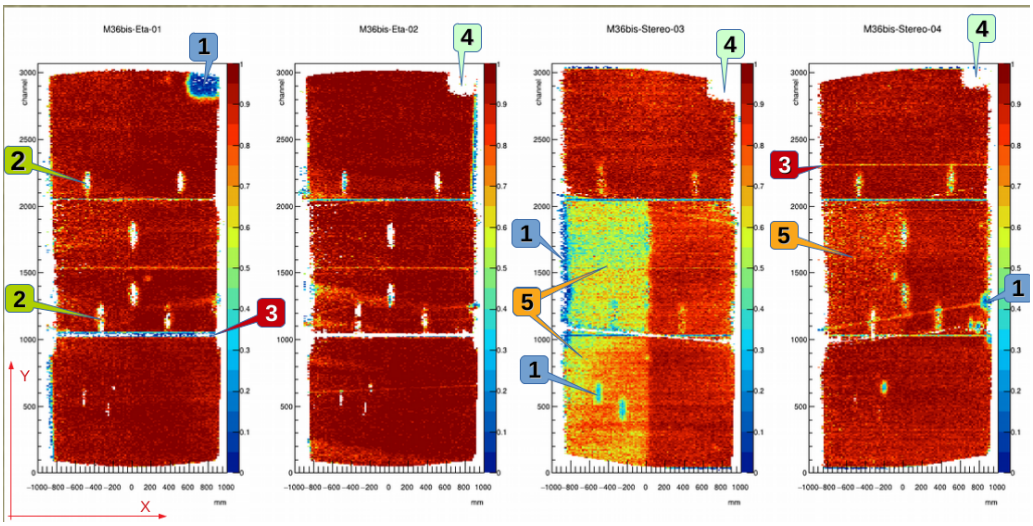

Figure 8: An example of module efficiency map.

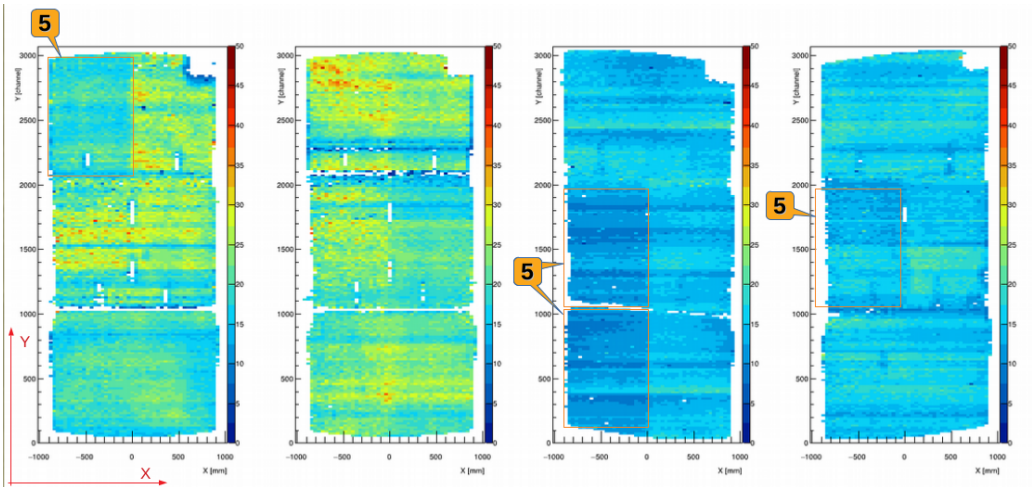

Figure 9: An example of module cluster charge map.

example of measured efficiency map for a module during cosmic tests is presented on Fig. 8, where numbers stand for:

1. Areas of observed discharges were passivated by Araldite™ or polyurethane glue.
2. Interconnections – mechanical insertions for module rigidity and gas exchange.
3. Artifacts of signal strips, shortcuts or cutoffs.
4. 'Ghost' areas with low statistics due to inefficiency in one of three other layers.
5. High voltage sectors with reduced potential, 550V for ST-03 and 570V for ET-01 and ST-04.

Collected cluster charge distribution in every (X, Y) bin of every detector layer is fitted with Landau p.d.f. The map of fit function most probable value parameter is drawn in addition to efficiency map. This provides extra information about gas charge amplification non-uniformity which is not observable in the areas with too high or too low efficiency.

The example of measured cluster charge map for a module is shown on Fig. 9. Cluster charge

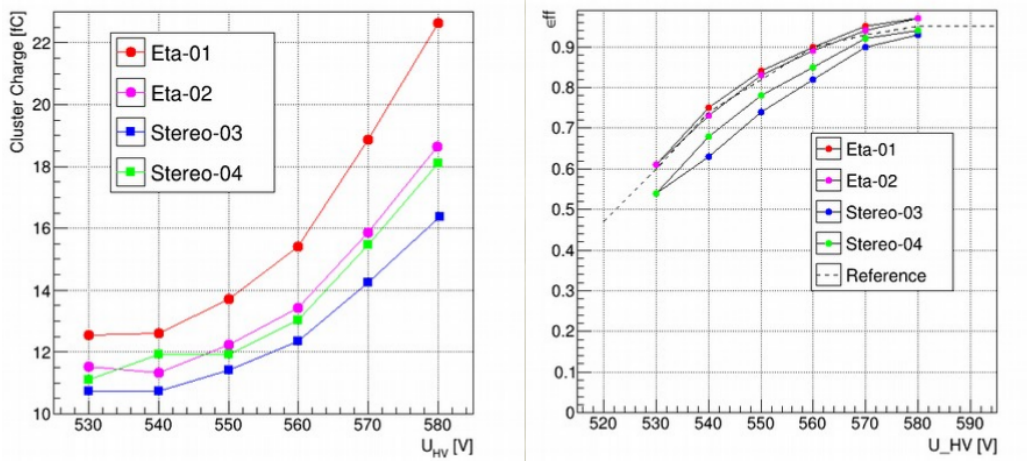

Figure 10: Cluster charge and efficiency dependence on high voltage.

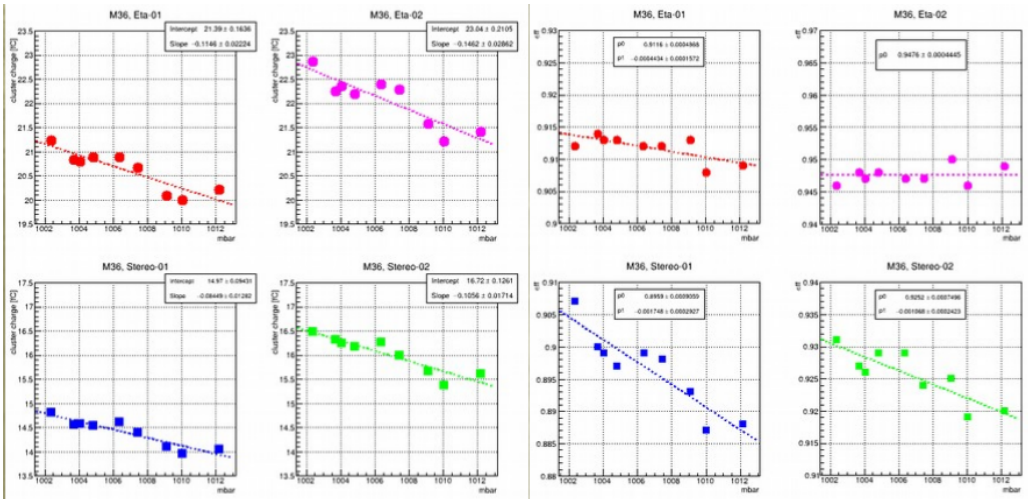

Figure 11: Cluster charge and efficiency dependence on atmospheric pressure.

on the colored palette of Z-axis is in fC (femtocoulombs). Signal amplitude is expected to have nearly exponential increase with high voltage, Fig. 10. Efficiency of a good layer is expected to increase with high voltage and then saturate around 90 – 98%. Reference curve was measured for Module-0 at CERN, atmospheric pressure conditions might be different.

MicroMegas modules operate at atmospheric pressure with a constant overpressure of $\approx$ 1 mbar to provide continuous gas flow. Gas gain depends on the electron mean free path so variations of measured signal amplitude with atmospheric pressure are expected and observed, see Fig. 11. Efficiency drop with pressure is observed on the level of $0.0 - 0.2\%/mbar$. Elevation above sea level in Dubna is 125m while in CERN at BB5 is 420m. This gives average pressure drop from Dubna to CERN about 33 mbar. To partially compensate for possible drop in efficiency cosmic tests in Dubna were done with increased high voltage +10V to nominal. So in terms of gas sparking modules have successfully passed tests in even more extreme conditions than in CERN.

5. Conclusions

A total of 33 LM2 modules were assembled and tested in JINR (Dubna) for ATLAS NSW Upgrade. Some of them were repaired then re-assembled again so that passed cosmic tests twice. For each layer of each module 2D maps of efficiency and cluster charge distributions have been produced. Effects of atmospheric pressure on cluster charge and efficiency are observed. The number of available ROCs was limited not allowing to test the whole module in a single step thus each readout board was installed and removed O(100) times. An installation method based on clearance measurements was developed giving repeatable results with only minor expert interventions. All of the 14 readout cards used for measurements remain operational.

Acknowledgments

The author thanks Theo Alexopulos and Christos Bakalis from CERN for guiding through readout electronics installation and operation principles. Also it was very pleasant experience to work with the Dubna modules construction team, in particular with Zaza Chubinidze, who supported the idea of taking clearance measurements during readout cards installation.

References

[1] The ATLAS Collab., *ATLAS New Small Wheel TDR*, CERN-LHCC-2013-006

[2] Y. Giomataris, P. Rebourgeard, J. P. Robert and G. Charpak, *MICROMEGAS: A High granularity position sensitive gaseous detector for high particle flux environments*, Nucl. Instrum. Meth. A **376** (1996), 29-35

[3] Balykina et.al, *Developing Production Technology and Control Methods for Micromegas Detectors*, PEPAN Letters, Vol. 18, No. 3, pp. 323–337 (2021)

[4] George Iakovidis for ATLAS Muon Collaboration, *VMM3, an ASIC for Micropattern Detectors*, proceedings of *MPGD2017* (2019)